Biophysical Chemistry 153 (2010) 61–69

Contents lists available at ScienceDirect

Biophysical Chemistry

journal homepage: http://www.elsevier.com/locate/biophyschem

Studies on solvatochromic properties of aminophenylstyryl-quinolinum dye, LDS 798, and its application in studying submicron lipid based structure

Pabak Sarkar [a,c,*], Rafal Luchowski [a,c], Sangram Raut [a,b], Nirupama Sabnis [c], Alan Remaley [d], Andras G. Lacko [c], Sanjay Thamake [b], Zygmunt Gryczynski [a,c], Ignacy Gryczynski [a,e,*]

[a] Center for Commercialization of Fluorescence Technologies, University of North Texas Health Science Center, Fort Worth, TX 76107, United States
[b] Department of Biomedical Sciences, University of North Texas Health Science Center, Fort Worth, TX 76107, United States
[c] Department of Molecular Biology and Immunology, University of North Texas Health Science Center, Fort Worth, TX 76107, United States
[d] Department of Laboratory Medicine, National Institute of Health, Bethesda, MD, United States
[e] Department of Cell biology and Anatomy, University of North Texas Health Science Center, Fort Worth, TX 76107, United States

ARTICLE INFO

Article history:
Received 17 September 2010
Accepted 4 October 2010
Available online 13 October 2010

Keywords:
Aminostyryl quinolinum dye
Fluorescence correlation Spectroscopy
Solvatochromism

ABSTRACT

The styryl group of dyes has been used in cellular studies for over 20 years because of their solvatochromic and/or electrochromic properties. Here we report characterization of solubility and solvatochromic properties of a near infra-red styryl dye, styryl 11 or LDS 798. We have extended our studies to small unilamellar vesicles and lipid based nanoparticles and found that solvatochromic properties of this dye used in tandem with fluorescence correlation spectroscopy can be used to efficiently determine the diffusion coefficient and hence the size of the submicron lipid based particles. This technique has the potential to provide essential information about liposomal and vesicular structures and their movement *in vitro* and *in situ*.

Published by Elsevier B.V.

1. Introduction

Styryl dyes have been investigated and used commercially for their solvatochromic/electrochromic properties. Their use as potentiometric dyes is well documented [1,2]. For more than a decade they have also been used to study vesicle trafficking and exocytosis [3,4]. The feature that makes styryl dyes attractive for membrane studies is their spectral response to local electric fields. Also, similar to other solvatochromic dyes, styryl dyes fluoresce strongly in a non-polar environment. They can thus be used as membrane markers in co-localization experiments.

Most of the styryl dyes used for fluorescence studies with biological samples have been aminostylyl pyridinium (ASP) derivatives. Typically, their alkylaminophenyl 'tail' is connected to electron withdrawing pyridinium 'head' group through conjugate bond(s). The tail is responsible for its membrane binding while the cationic head group determines its membrane permeability. The spectral properties are determined generally by the number of aromatic rings and the conjugate bonds that join them [3]. In an aqueous environment, the dielectric properties of water induce high non-radiative decay rates and thus render the molecule non-fluorescent. The free movement of the dye can also lead to increase in non-radiative decay [5]. Once the polarity decreases, the radiative decay becomes substantial and this results in a detectable fluorescence signal. Though there are other factors, including aggregation of the dye in water and charge shift of the dye in the excited state, that may contribute to the spectral characteristics of the dye, solvatochromism still exerts a major impact on the dye's spectral properties [2].

Styryl-11 or LDS 798 (*1-Ethyl-4-(4-(p-Dimethylaminophenyl)-1,3-butadienyl)-quinolinum percholate*) is a styryl compound that contains monocationic quinolinum group instead of the pyridinium group of ASP dyes and has a rather short dialkylaminophenyl 'tail' region [6]. In ethanol its peak absorption is at 580 nm and peak emission is at 770 nm making it a useful near infra-red dye. Near infra-red solvatochromic dyes have been shown to be useful for studying tissues in-vivo [7]. LDS 798 has been used as a laser dye and has a very weak fluorescence in aqueous solution (quantum yield of 0.002 [8]). Previous studies have shown that LDS798 has a very short fluorescence lifetime in water (<20 ps) while its lifetime increases in ethanol and in polymer films [9]. Stoke's shifts have been found to be higher in water than in ethanol. The purpose of this study was to characterize the solvatochromic properties of this aminophenyl styryl quinolinum (ASQ) dye and compare these features with those of established (well studied) ASP dyes. Recent studies on the structure and fluorescence properties of ASQ dyes indicate that their quinolinum group acts as the electron acceptor while the aminophenyl group acts as the electron donor [10]. Our studies show that styryl-11 (LDS 798) retains all the solvatochromic

* Corresponding authors. Sarkar is to be contacted at the Center for Commercialization of Fluorescence Technologies, Department of Molecular Biology and Immunology, University of North Texas Health Science Center, 3500 Camp Bowie Boulevard, Fort Worth, TX 76107, United States. Tel.: +1 11 817 735 0148; fax: +1 11 817 735 2118. Gryczynski, Department of Cell Biology and Anatomy, University of North Texas Health Science Center, 3500 Camp Bowie Boulevard, Fort Worth, TX 76107, United States. Tel.: +1 11 817 735 5471; fax: +1 11 817 735 2118.
E-mail addresses: psarkar@live.unthsc.edu (P. Sarkar), ignacy.gryczynski@unthsc.edu (I. Gryczynski).

0301-4622/$ – see front matter. Published by Elsevier B.V.
doi:10.1016/j.bpc.2010.10.005

properties of ASP and ASQ dyes. The studies described here also indicate that LDS 798 might integrate into the bilayered lipid membrane in multiple orientations due to its bulky aromatic head region and short alkyl tail region.

With the recent advent of advanced fluorescence based technologies, including fluctuation correlation spectroscopy, fluorescence lifetime imaging, generalized polarization microscopy and single molecule detection, styryl dyes can be used to obtain detailed information on complex systems. Solvatochromic dyes, like Lauradan, are being extensively used for correlation spectroscopy and generalized polarization studies of lipid membranes [11] while lifetime based imaging using this group of dyes has a potential to be used for probing excitable cell/tissue samples. One of our goal was to investigate how LDS798 solvatochromism can be used with the modern fluorescence techniques for probing systems of biomedical significance. Thus, we investigated the potential application of LDS 798 to determine the dimensions and movement of submicron lipid-based structures using fluorescence correlation spectroscopy (FCS) that has already been used to study the dynamics of cellular and subcellular structures [11,12]. FCS is markedly more sensitive than similar fluorescence based techniques like fluorescence recovery after photobleaching (FRAP) or fluorescence loss in photobleaching (FLIP). The findings obtained using FCS analysis with LDS 798 fluorescence show that this approach may be particularly appropriate for labeling the lipid based submicron structures and the study of their dynamics.

2. Materials and methods

LDS 798 was purchased from Exciton (Dayton, OH) and used without any further purification. 1,4-dioxane, ethyl acetate, dichloromenthane (DCM), 1-octanol, ethanol, methanol, N,N-dimethyl formammide (DMF), dimethyl sulfoxide (DMSO) were purchased from Sigma-Aldrich or Fluka (St. Louis, MO). 1-Butanol, 2-propanol, acetonitrile and chloroform were purchased from Fisher Scientific (Pittsburgh, PA). All the solvents were spectrphotometric grade. Deionized water used for the experiments was from Millipore distillation system. 1,2-dimyristoyl-*sn*-glycero-3-phospho-(1′-rac-glycerol) (DMPG), 1,2-dimyristoyl-*sn*-glycero-3-phosphocholine (DMPC) was purchased from Avanti polar lipids (Alabaster, AL). sodium dodecyl sulfate (SDS) powder and Triton-X-100 was from Sigma-Aldrich (St. Louis, MO).

2.1. Preparation of phosopholipid bilayers and high density lipoprotein-like nanoparticles

For SUV preparation, stock solution of lipids was prepared in chloroform.

Lipid films were prepared by evaporating the chloroform in inert environment under steady flow of Argon gas. Lipid films were then hydrated with phosphate buffered saline supplemented 500 μM EDTA. After hydration, the samples were sonicated till clarity with 2 minute pulses of sonication with ultrasonic processor UP200H system (Hielscher Ultrasonics GmbH, Germany) followed by resting phase in ice.

The cholate dialysis procedure used, was based on the procedures described for discoidal rHDL particles [13–15]. A mixture of Egg yolk phosphatidyl choline (15 mg), free cholesterol (0.35 mg) and cholesterol oleate (0.15 mg) all in chloroform were dried down under nitrogen. Apo A-1 (5 mg) or ApoA1-mimetic 5A peptide (1 mg) and 3% DMSO were mixed. 14 mg sodium cholate was added and volume was made up to 2 ml with buffer (10 mM Tris, 0.1 M KCl, 1 mM EDTA pH 8.0). The mixture was incubated overnight at 4 °C.

The mixture was then dialyzed against 2 liters of 1X phosphate buffered saline for 48 h with change of buffer every 2 h on the first day, (at least) 3 times and later kept overnight. The mixture was centrifuged for a quick spin and then sterilized by passing through 0.45 μM filter.

The hydrodynamic volume of these SUVs and nanoparticles was estimated using dynamic light scattering Nanotrac Particle Size Analyzer (Nano Track; ISee imaging systems, Raleigh, NC).

2.2. Spectroscopic studies and mathematical models

Extinction coefficient of LDS 798 in ethanol was reported by the manufacturer [6]. Equal amount of LDS 798 was dissolved in equal volume of ethanol, octanol and water. Then, samples were diluted to various concentrations and optical densities were measured in Cary 50 Bio (Varian Inc., Australia) spectrophotometer. The absorptions were plotted as a function of concentration calculated using extinction coefficient of LDS 798 in ethanol.

Partition coefficient (log P) was measured by shake-flask method [16]. In brief, supersaturating the mixture of 1:1 water:octanol with LDS 798 was shaken vigorously at room temperature (~20 °C) overnight and 500 ul aliquots were taken from both water and octanol phase. The aliquots were diluted with their respective solvents and absorption was measured.

For steady state fluorescence spectroscopic measurements, Cary Eclipse spectrofluorometer (Varian Inc., Australia) was used. In most of the measurements the samples were excited with 530 nm light and a 570 nm long-pass filter was used before the detector to minimize the effect due to scattering. For some measurements, like that with small unilamelar vesicles (SUV)s, excitation of 470 nm was used and 530 long-pass filter was used at observation in those cases. Absorption of each sample at 530 or 470 nm were used to correct the difference in fluorescence intensity due to variable excitation. All the samples used had an optical density less than 0.2, but greater than 0.02 at 530 nm. For absorption measurements with SUVs, the scattering due to them was measured and subtracted from the absorption values.

Quantum yield was calculated with cresyl violet in ethanol (quantum yield 0.54) as reference solution, using the equation

$$Q = Q_R \frac{I^* abs_R n^2}{I_R^* abs\, n_R^2} \tag{1}$$

Where, Q and Q_R are quantum yields of the sample and reference, I and I_R are the fluorescence intensities area under the curve for the sample and reference, abs is the absorption of the samples at the wavelength that was used to excite the samples and n is the refractive index of the solvents.

For Lippert–Mataga (LM) plot following equations were used to calculate the orientation polarizability, Δf.

$$\Delta f_{LM} = \frac{\varepsilon - 1}{\varepsilon + 2} - \frac{n^2 - 1}{2n^2 + 1} \tag{2}$$

Where, ε is the bulk dielectric permittivity.

Simplified Bilot–Kawski (BK) equations were also used to calculate orientation polarizability and the ratio of excited and ground state dipole moment with following equations

$$f_{BK}(\varepsilon, n) = \frac{2n^2 + 1}{n^2 + 2}\left(\frac{\varepsilon - 1}{\varepsilon + 2} - \frac{n^2 - 1}{n^2 + 2}\right) \tag{3}$$

$$g_{BK}(n) = {}^3/_2 \frac{n^4 - 1}{(n^2 + 2)^2}$$

$$\Phi_{BK}(\varepsilon, n) = f_{BK}(\varepsilon, n) + g_{BK}(n) \tag{4}$$

$$\begin{aligned} \tilde{\nu}_A - \tilde{\nu}_F &= m_1 \cdot f_{BK}(\varepsilon, n) + const \\ \tilde{\nu}_A + \tilde{\nu}_F &= m_1 \cdot \Phi_{BK}(\varepsilon, n) + const \end{aligned} \tag{5}$$

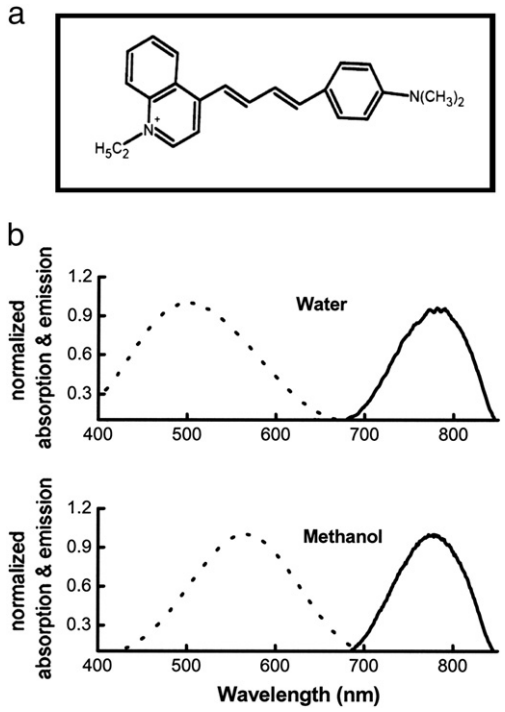

Fig. 1. Initial indications about solvatochromic property of LDS 798. Chemical structure of LDS 798 (styryl-11) (a). Absorption (dotted line) and emission spectra (continuous line) of LDS 798 in ethanol (top) and water (bottom) (b).

$$\frac{\mu_e}{\mu_g} = \frac{m_1 + m_2}{m_2 - m_1} \tag{6}$$

For lifetime measurements, FluoTime 200 (PicoQuant GmbH, Germany) time domain spectrofluorometer was used. This spectrofluorometer contains cooled multi-channel plate detector (Hamamatsu, Japan) and is accessorized with a monochromator at the observation. 470 nm laser diode (LDH-PC-470) was used as the excitation source. This laser diode has a pulse width of <70 ps. The fluorescence decays were fitted with FluoFit version v-4.0 software (PicoQuant GmbH, Germany) using multiexponential deconvolution model

$$I(t) = \int_{-\infty}^{t} IRF(t') \sum_i \alpha_i e^{-\frac{t-t'}{\tau_i}} \tag{7}$$

Where IRF (t′) is the instrument response function at time t′, α is the amplitude of the decay of the ith component at time t and τ_i is the lifetime of the ith component.

Radiative and non-radiative rate constants for LDS 798 in different solvents using following equations

$$Q = \frac{\Gamma}{\Gamma + k_{nr}} \tag{8}$$

$$\tau = \frac{1}{\Gamma + k_{nr}} \tag{9}$$

2.3. Fluorescence lifetime correlation spectroscopy studies

The data for fluorescence lifetime correlation spectroscopy (FLCS) experiments was collected with MicroTime 200 confocal microscope (PicoQuant GmBh, Germany). The methodology using these studies has been described earlier [17]. Briefly, pulsed light from 470 nm solid state laser was focused 10 μm above the cover-slip surface, but inside the drop of the sample solution. 20 μW laser light power for all the FLCS experiments was used. Separate measurements characterizing microscope/objective alignment and features for the confocal volume was performed. For the purpose of confocal volume characterization, 3D raster scanning of fluorescence nanospheres was applied [18,19] that yielded a value of 0.16 fl. Olympus IX71 inverted microscope and Olympus UPlanFL N 100× magnification oil objective, NA = 1.3 was used for the measurements (fluorescence fluctuations). The scattered light was filtered with sets of filters (500 long wavelength pass and 473 RazorEdge, Semrock). Filtered light was focused through 30 μm pinhole to single photon avalanche photodiode (SPCM-AQR-14, Perkin Elmer). Data analysis was performed with SymPhoTime (v. 5.0) software (Picoquant, Germany) and autocorrelation function was defined according the formula:

$$G(\tau) = \frac{\langle \delta I(t) \delta I(t+\tau) \rangle}{\langle \delta I(t) \rangle \langle \delta I(t+\tau) \rangle} \tag{10}$$

Where $\delta I(t)$ and $\delta I(t+\tau)$ are the fluorescence intensity fluctuations from the mean at time t and $t+\tau$, respectively. Auto-correlation curves due to translational diffusion through 3-dimentional Gaussian shaped volume were fitted with following formula [2,3]:

$$G(\tau) = \sum_{i=1}^{n} \rho_i \left(1 + \frac{\tau}{\tau_{Di}}\right)^{-1} \left(1 + \frac{\tau}{\tau_{Di}\kappa^2}\right)^{-1/2} \tag{11}$$

where ρ_i is a contribution of ith diffusion species for total autocorrelation function, τ_{Di} is a diffusion time of ith diffusion species, κ is length (z_o) to diameter (w_o) of the focal volume. On the basis of

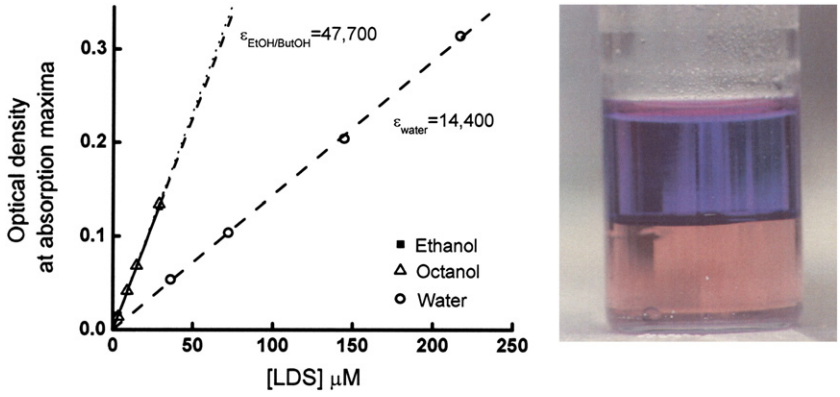

Fig. 2. After factoring its low extinction coefficient in water it was found that LDS 798 partitions adequately in water. Extinction coefficient of LDS 798 in different solvents (a). Partition coefficient of LDS 798 (b).

Table 1
List of solvents, their dielectric constants and refractive indices, solubility profile and, fluorescence properties (spectral shift, quantum yield and average lifetimes) of LDS 798 when it was dissolved in them.

Solvent	Dielectric constant	Refractive index	$\nu_{Abs} - \nu_{Em}$ cm^{-1}	% quantum yield	Average lifetime (ps)
Aprotic					
Dioxane	2.21	1.42	4541.56	3.06	206
Ethyl acetate	6.02	1.37	4903.10	2.02	223
Acetonitrile	36.6	1.34	5265.30	0.23	85
DMF	38.3	1.43	5243.48	0.35	126
DMSO	47.2	1.48	5195.84	0.42	176
Protic					
1-Octanol	10.3	1.43	3426.79	6.11	562
1-Butanol	17.85	1.40	3950.73	2.75	330
n-Propanol	21.65	1.39	4126.76	1.34	205
Ethanol	24.3	1.35	4427.06	0.76	147
Methanol	33.1	1.33	4793.78	0.30	78
Outlier					
Chloroform	4.98	1.45	3108.66	3.21	815
DCM	8.93	1.42	2807.91	3.52	712
Water	78.3	1.33	7205.81	0.08	<50

the fit to the autocorrelation function we determined also the diffusion coefficient D according:

$$D = \frac{w_o^2}{4\tau_D} \tag{12}$$

3. Results and discussion

Styryl dyes have been used extensively for studying membrane dynamics and changes in membrane potential. The aminostyryl pyridinium sub group has also been be successfully used to probe the dynamics of vesicle trafficking in an activity dependent manner [3].

3.1. Solvatochromic characterization of LDS 798

LDS 798 or styryl-11 contains a quinolinum 'head' region which is connected to the dimethylaminophenyl 'tail' via two alternate double bond structures (Fig. 1 top). This structural configuration is quite distinct from that of other well known styryl dyes. While the overall configuration of LDS 798 retains the features responsible for its spectral properties, it has a very short (dimethyl) tail and a bulky (quinolinum) and monocationic head region that is unique to most of the commercially available styryl dyes. In our previously published study, we have observed the difference in Stoke's shift of LDS spectra with ethanol and aqueous medium (Fig. 1 bottom) that led us to study the solvatochromic properties of LDS 798.

Current studies were initiated with qualitative characterization of LDS 798 solubility in solvents of varying polarity and showed that it is weakly soluble or insoluble both in highly hydrophobic solvents like cyclohexane and hydrophilic aqueous solutions. It was noticed that LDS 798, though dissolved slowly in deionized water, was totally insoluble in cyclohexane even after vigorous overnight shaking.

During study of spectral properties of LDS 798, the absorption spectrum was blue shifted in water without any significant spectral broadening (Fig. 1 bottom) ruling out the possibility of LDS 798 self-aggregation. The study of the extinction coefficient of LDS 798 in octanol and water (Fig. 2 left) showed that the extinction coefficient in water deviated significantly from that value reported by the manufacturer (with ethanol as solvent) [6]. Partition experiments, using the shake-flask method and calculated extinction coefficients for LDS in water and octanol, yielded a log P of 0.54 indicating that LDS 798 dissolves in water reasonably well.

To understand the spectral changes due to solvatochromic properties of LDS 798, absorption and emission spectra were measured in solvents of various polarity and refractive indices (Table 1). Next, the Stoke's shift ($\nu_{abs} - \nu_{Em}$ in cm^{-1}) was plotted for each solvent as a function of their respective polarity function. Both Lippert–Mataga (LM) and simplified Bilot–Kawski (BK) models were used to fit the data (Fig. 3) and characterize the solvent effect. Both models indicate that the Stoke's shift change was correlated with the polarity function in aprotic solvents. However, a major observation from these plots was that protic and aprotic solvents both show completely different patterns of Stoke's shifts. This deviation of protic

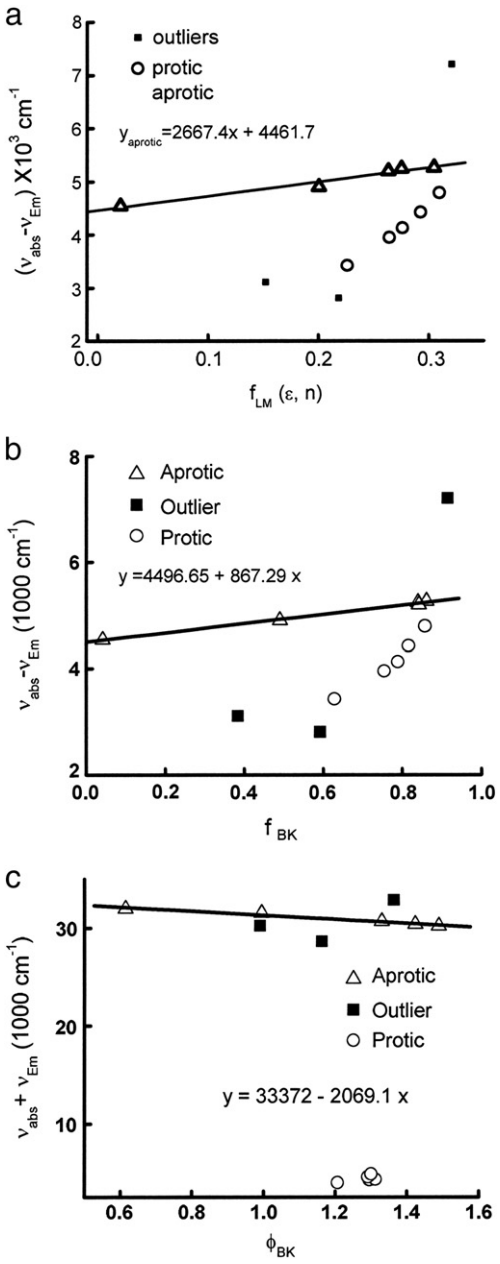

Fig. 3. Solvent relaxation pattern of LDS 798. a) The difference of absorption and emission maxima was plotted as a function of Lippert–Mataga parameter f_{LM} (ε, n). b) The difference of absorption and emission maxima was plotted as a function of Bilot–Kawski parameter f_{BK}(ε, n) and c) the sum of absorption and emission maxima was plotted as function of Bilot–Kawski parameter Φ(ε, n). The protic and aprotic solvent showed a difference in magnitude of solvent relaxation.

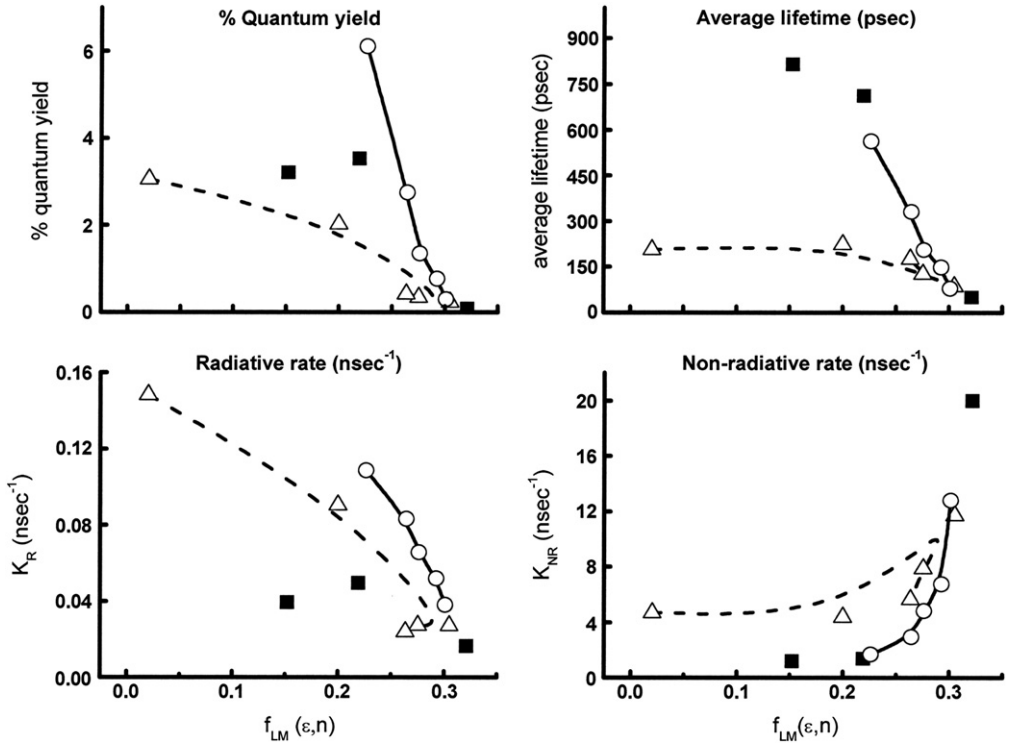

Fig. 4. Solvent induced changes in radiative rates of LDS 798. (Top) The change in quantum yield and fluorescence decay lifetime with change in Lippert's function of dielectric. (Bottom) Non-radiative and fluorescence decay of LDS 798 with change in Lippert's function of dielectric. Δ indicates aprotic solvents, ○ indicates protic solvents and ■ indicates outliers.

solvents has been associated with their tendency hydrogen bonding, aggregation or other specific interaction with the fluorophore [5]. Stoke's shift of LDS 798 in alkyl halides, chloroform and dichloromethane, could not be fitted with protic or aprotic profile in both LM and BK model, suggesting that there might be some specific interactions taking place between the solute and solvent that cannot be taken in to account by these models. Using Bilot–Kawski model and considering that both ground state and excited state dipole moments are parallel, we calculated the excited state dipole moment as 2.44 fold larger than the ground state dipole moment.

For understanding the radiative changes due to solvatochromic fluorescent properties of LDS 798, we measured its quantum yield in different solvents with cresyl violet in ethanol as the reference solution Fig. 4 (top left). We also measured the fluorescence lifetime of LDS 798 in different solvents (Fig. 4 top right). LDS 798 has a maximum quantum yield of ~6% in octanol, whereas its quantum yield was lowest in water (<0.1%). The fluorescence decay profiles showed that the maximum average lifetime was in the sub-nanosecond range (maximum 814 ps in chloroform and <25 ps in water). Radiative and non-radiative rate constants calculated from quantum yields and fluorescence lifetime (Fig. 5 bottom) show that the non-radiative rate constants are two orders of magnitude larger than the radiative decay explaining the major Stoke's shift seen with LDS 798. All these parameters were plotted as a function of LM parameter of polarity (*f*). The response from protic solvents was distinctly different from that of aprotic solvents and this further indicates that H-bonding might have a significant effect in LDS798 spectra and fluorescence intensity (Fig. 5). As observed earlier, LDS 798 fluorescence response was distinctly different in alkyl halide solvents when compared with that of other aprotic solvents.

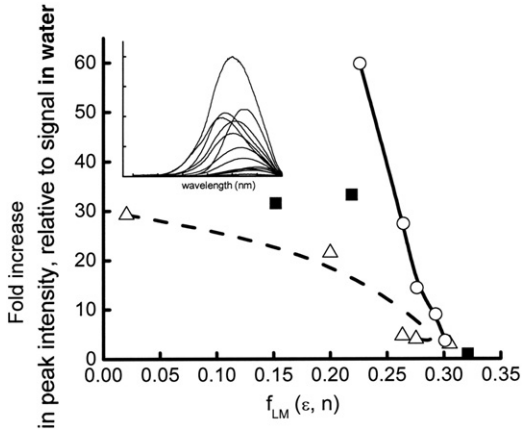

Fig. 5. Effect of polarity on the peak intensity of LDS 798. (Inset) Spectral data of LDS 798 fluorescence in various pure solvents. (Main plot) The peak intensity was plotted with Lippert–Mataga function for protic (o), aprotic (Δ) and other (■) solvents.

The spectral properties of LDS798 determined here are in good agreement with that of reported ASQ dyes [10]. Its absorption spectrum is blue shifted in polar solvent, like water, as seen in other ASQ dyes. The Bilot–Kawski and Lippert–Mataga plots for solvent relaxation show that the Stoke's shift increases linearly as a function of orientation polarizability. The key observation reflected in the plot is the response of aprotic solvents compared with protic solvents. This has been attributed to the formation of hydrogen bonds between the solute and solvent, observed in other systems [5]. Both Lippert–Mataga and Bilot–Kawski models failed to explain the effect of the Stoke's shift in alkyl halide solvents and water indicating that there might be some other specific interactions in addition to polarizability. Significant red shift in fluorescence spectra with increase in solvent polarity indicates that the excited singlet state is stabilized in polar solvents.

3.2. Spectral and radiative changes of LDS 798 fluorescence in micelles and liposomes

After characterizing the spectral and radiative properties of LDS 798 in solvents with different polarity, studies were performed on its

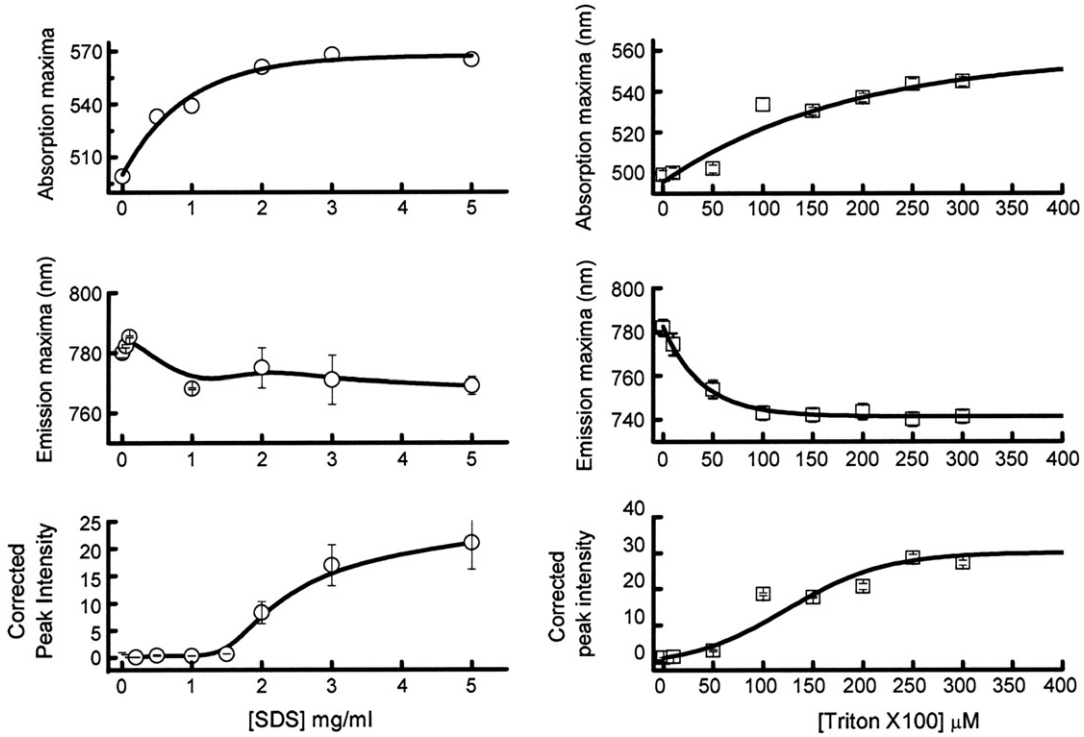

Fig. 6. Effect of detergents on the fluorescence signal of LDS 798 in aqueous solution. Addition of detergent in aqueous solution of LDS 798 resulted in red shift of absorption maxima (top panels), blue shift in emission maxima (middle panel) and increase of fluorescence intensity (bottom panels).

fluorescence properties in the presence of amphipathic molecules, dissolved/dispersed in aqueous medium (Fig. 6). Amphipathic molecules like detergents and phospholipids create a hydrophobic environment in aqueous media. These compounds have been used extensively to study fluorescent properties of other styryl dyes and have laid the foundation for their use in studying cellular events [2].

Spectral properties (both absorption and emission) of LDS 798 were measured while titrated with sodium dodecyl sulfate (SDS—an ionic detergent) and Triton-X 100 (a non-ionic detergent) at room temperature. These studies reveal that absorption maxima shifted to the longer wavelengths upon addition of both SDS and Triton-X100. The fluorescence spectral analysis showed a progressive blue shift with increasing concentration of Triton-X 100 but not with SDS. The intensity of fluorescence increased with addition of detergents (both SDS and Triton-X 100). This increase was found to be phase dependent as the LDS fluorescence signal increased once the critical micellar concentration was attained (8.2 μM for SDS and 200 μM for Triton-X-100) and leveled off after stable micellar structure was attained (at higher concentrations of detergent). This observation is consistent with reports based on the study of the polymerization of styryl dyes [20] that have reported spectral shift in fluorescence decreased once nucleation of polymerization was attained.

Study of spectral and radiative properties of styryl dyes in unilamellar vesicles (mean diameter ~60 nm; Table 2), prepared with neutral phospholipids (DMPC) and negatively charged phospholipids (DMPG) showed a red shift in absorption and a blue shift in emission spectra upon addition of unilamellar vesicles to the dye. Two emission peaks (at 550 nm and 720 nm) in presence of SUVs was observed when excited with 530 or 470 nm light (Fig. 7). When excited with even longer wavelength (620 nm) only one peak at ~740 nm was observed while the LDS 798 fluorescence attained saturation at lower concentrations of DMPG than DMPC (Fig. 7, lower panels).

Finally, polarity dependent changes in LDS 798 fluorescence in reconstituted high density lipoprotein (HDL) nanoparticles (rHDL) were measured to see whether this phenomenon can be applied to characterization of nanoparticles used in drug delivery. These nanoparticles were shown to have a mean diameter of <20 nm (Table 2) and contained egg yolk phosphatidyl choline, cholesterol, cholesteryl oleate and either apolipoprotein A-I protein (in rHDL) or an apolipoprotein mimetic peptide (termed as 5A peptide in the figures). These polypeptide components are required for structural integrity of the synthetic/reconstituted lipoprotein particles. Addition of rHDL (containing either apo A-I or the 5A peptide) in aqueous solution of LDS 798 led to a mild red shift in absorption spectra and strong blue shift in emission spectra (Fig. 8). The fluorescence intensity increased upon addition of the respective nanoparticles to the dye. The change in fluorescence spectrum of LDS 798 in presence of rHDL and peptide nanoparticles suggest alterations in their surface charge, perhaps due to conformational change in the polypeptide components as the lipid ingredients of both preparations were identical.

Ensemble studies show that amphipathic molecules influence the spectral properties and radiative rates of LDS 798. Most of the amphipathic molecules induced a red shift in absorption spectra while in all the cases the fluorescence spectra was blue shifted and the peak intensity increased by different magnitudes. In reconstituted

Table 2
Size distribution, Diffusion coefficient and detected concentrations of the lipid based small unilamelar vesicles and nanoparticles.

Sample	Size distribution (nm)	Diffusion coefficient ($\mu m/s^2$)	Detected concentration (nM)
Free LDS 798	–	199 ± 25	
SUVs (pure)			
DMPC	55.4 (98%)	3.28 ± 0.5	19.1
	2100 (2%)		
DMPG	56.4 (96%)	3.79 ± 1.1	0.25
	295 (4%)		
Nanoparticles (mixed lipids)			
rHDL NP	43 (100%)	2.0 ± 0.3	15.2
Peptide NP	34 (100%)	3.1 ± 0.5	11.1

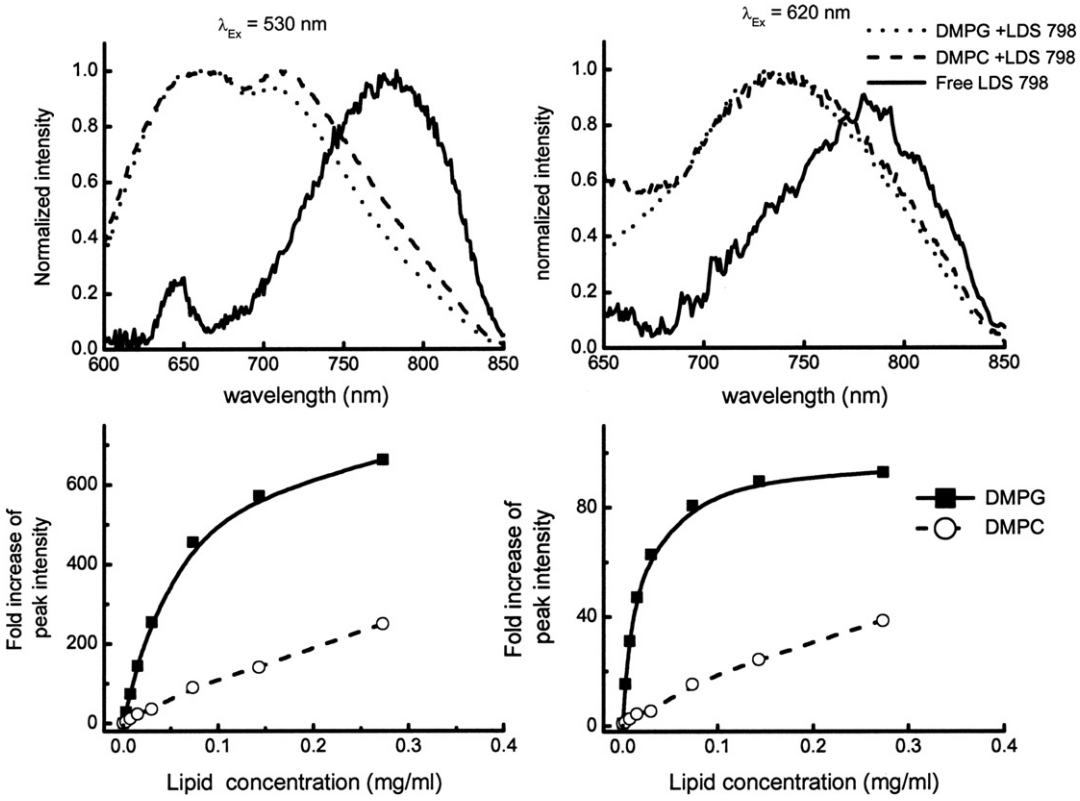

Fig. 7. Spectral and radiative changes in LDS 798 fluorescence on addition of bilayered membrane. (Top) Normalized spectra of free LDS 798 (continuous line) and LDS 798 in presence of DMPC (dashed lines) or DMPG (dotted lines) with 530 nm (left) and 620 nm (right) excitation. (Bottom) Fold change in LDS 798 fluorescence at peak intensities on addition of lipid membranes.

bilayered structures, always two peaks were observed. This observation is previously unreported. Unpublished initial studies from our laboratory for these samples indicate, that there might be two populations with distinct excitation peaks. Molecular phenomenon leading to this observation and its significance is not yet clear and would require further study. The saturation profile of LDS798 fluorescence with DMPC and DMPS suggest that fluorescence properties of LDS 798 are enhanced when it interacts with the negatively charged or polar residues or conversely, LDS 798 might not interact effectively with the neutral phospholipids as compared with polar/negatively charged lipids. Both these possibilities might be true as previous reports have shown that styryl dyes have enhanced fluorescence properties under mildly acidic condition.

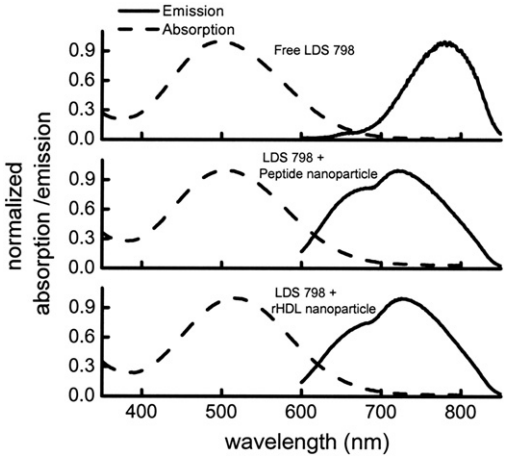

Fig. 8. Effect of HDL and HDL-like nanoparticles on LDS 798 fluorescence. Addition of nanoparticles resulted in slight red shift of absorption maxima and strong blue shift of emission maxima. Two peaks were observed in the fluorescence spectra after addition of nanoparticles to aqueous solution of LDS 798.

3.3. Fluorescence correlation spectroscopy studies on LDS 798

Small log P value of LDS 798 and manifold increased quantum yield of LDS 798 in non-aqueous solvents prompted us to hypothesize that in an aqueous solution with SUV, LDS 798 fluorescence will preferentially be associated with the nanoparticles as the signal generated by these associated LDS 798 molecules will be stronger than the LDS 798 molecules in the aqueous phase. Thus, LDS 798 fluorescence signal can be used to characterize the diffusion of these submicron particles. The diffusion pattern of LDS 798 molecules associated with the nanoparticles will thus correspond to that of the particles themselves and will be significantly different from those that are free (and weakly fluorescent). We decided to test the hypothesis using single point fluorescence lifetime correlation spectroscopy. Figs. 9 and 10 shows the correlation profile and the burst profile of the measurements. Table 2 shows the average number of particles and the diffusion coefficient of LDS 798 in pure phospholipid vesicles (Fig. 9), reconstituted rHDL and nanoparticles with reconstituted 5A peptide (Fig. 10). The FCS results were in agreement with dynamic light scattering results measured independently (Table 2). The traces measured, showed very high fluctuations (Fig. 9, left) corroborating that correlation originated from the phospholipid vesicle bound LDS 798 molecules. The signal from the Free LDS 798 in water was very weak and was characterized by poor correlation and fast diffusion rates typical of free dyes (Fig. 10). The smaller HDL-like particle was observed to have a relatively slow diffusion rate. However, this trend was consistent in all 3 sets of experiments performed. This decrease in diffusion might be due to the incorporation of ApoA-I or the mimetic peptide that increases the density of the particle and slows down its Brownian motion. These results indicate that FCS can be used to study

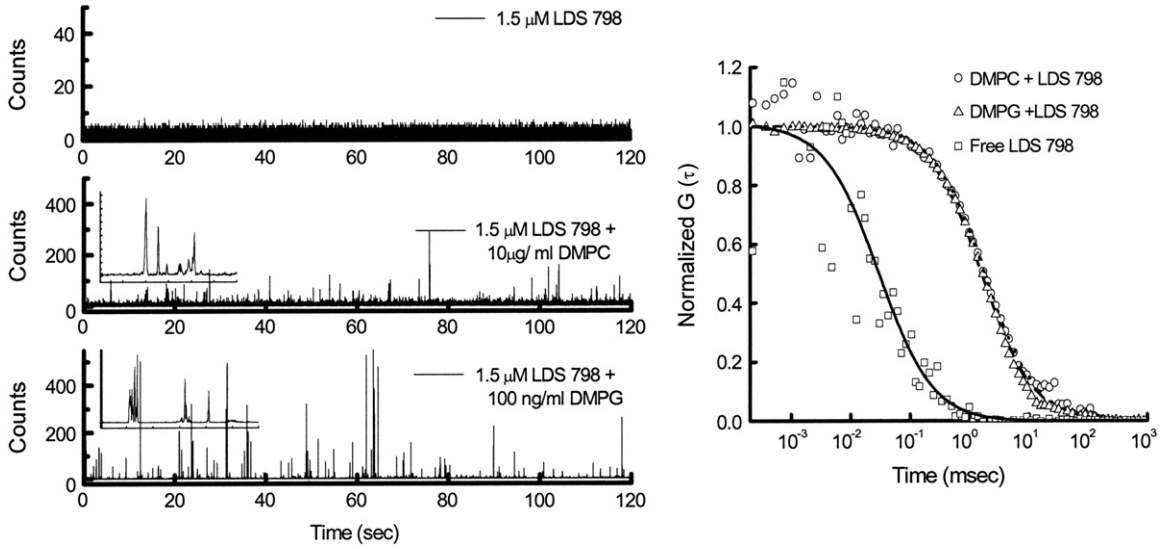

Fig. 9. Fluorescence correlation pattern of pure lipid SUVs. MCS traces of the measurements are shown in the left panels and normalized correlation pattern of LDS 798 fluorescence fluctuations is shown in the left panel.

the diffusion, and hence size, of the submicron lipid structures using solvatochromic fluorescence properties of LDS 798.

Fluorescence correlation studies with LDS 798 dyes indicate that it can be used to study hydrophobic structures with relatively easy staining protocol. Advanced correlation techniques have been developed and can be used to study aggregation pattern inside a cell. On the other hand, styryl dyes have been used to study exocytosis and other vesicle related phenomenon. Hence we anticipate that advanced correlation spectroscopy using styryl dye labeling can play a critical part in understanding the mechanism of vesicular transport dynamics. Long wavelength dyes like LDS 798 have an added advantage as the auto fluorescence background signal is negligible in the near-infra-red range. Though we have not checked the toxic effects of LDS 798, it has been reported for ASP dyes that concentrations below micromoles are not toxic for the cells up to 8–10 h after labeling [4].

Membrane localization and orientation of this subgroup of dyes has been very carefully linked to its structure. The structure of LDS 798 is very similar the ASP dyes. The major difference is in the head region, which contain a quinolinum ring rather than pyridinium. The tail region of LDS 798 is very short and contains dimethyl group. For ASP dyes this short tail generally leads to membrane permeabilization. The log P value and solubility profile of LDS 798 suggests that it can be soluble in aqueous media too. Thus, we believe LDS 798 might be useful in staining intracellular organellar membranes. Its localization in sub-cellular structures can be very interesting.

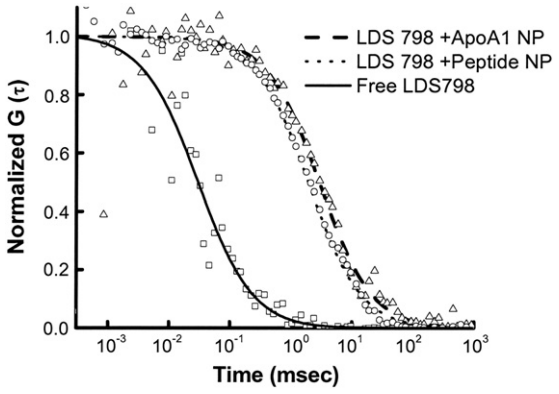

Fig. 10. Characterization of the dimensions of the HDL and HDL-like nanoparticles using FCS.

4. Conclusion

LDS 798 is a styryl group dye with near infra-red fluorescence. Its structure and fluorescence properties indicate that its radiative rate is dependent upon the micro-domain polarity among other factors. Our studies show that this can be conveniently used for FCS measurements of lipid based particles smaller than optical resolution. The concept of studying trafficking patterns of lipid structures using styryl dyes and FCS is novel and can provide insights in vesicle transport and release in cytological studies.

Acknowledgements

This work was supported by the Texas Emerging Technology Funding grant (given to the Center for Commercialization of Fluorescence Technology). ST was funded by a predoctoral fellowship (BC093521) DOD Breast Cancer Research Program (SIT). We would also like to thank Dr. Jamboor K. Viswanatha for allowing us to use the NanoTrack dynamic light scattering instrument and sonication system; Dr. Thomas Just Sørenson, for helping with solvent relaxation studies; and Dr. Badri Prasad Maliwal and Dr. Valeriya Trusova for the SUV preparation.

References

[1] C. Xu, L.M. Loew, The effect of asymmetric surface potentials on the intramembrane electric field measured with voltage-sensitive dyes, Biophys. J. 84 (2003) 2768–2780.
[2] E. Fluhler, V.G. Burnham, L.M. Loew, Spectra, membrane binding, and potentiometric responses of new charge shift probes, Biochemistry (N. Y.) 24 (1985) 5749–5755.
[3] W.J. Betz, F. Mao, G.S. Bewick, Activity-dependent fluorescent staining and destaining of living vertebrate motor nerve terminals, J. Neurosci. 12 (1992) 363–375.
[4] W.J. Betz, F. Mao, C.B. Smith, Imaging exocytosis and endocytosis, Curr. Opin. Neurobiol. 6 (1996) 365–371.
[5] J.R. Lakowicz, Principless of Fluorescence Spectroscopy, 2nd Ed.Kluwer Academic / Plenum Publisher, New York, 1999.
[6] U. Brackmann, Lambdachrome Laser Dyes Data Sheets, 1994.
[7] M.Y. Berezin, H. Lee, W. Akers, S. Achilefu, Near infrared dyes as lifetime solvatochromic probes for micropolarity measurements of biological systems, Biophys. J. 93 (2007) 2892–2899.
[8] R. Luchowski, Z. Gryczynski, P. Sarkar, J. Borejdo, M. Szabelski, P. Kapusta, et al., Instrument response standard in time-resolved fluorescence, Rev. Sci. Instrum. 80 (2009) 033109.
[9] R. Luchowski, P. Sarkar, S. Bharill, G. Laczko, J. Borejdo, Z. Gryczynski, et al., Fluorescence polarization standard for near infrared spectroscopy and microscopy, Appl. Opt. 47 (2008) 6257–6265.
[10] B. Jędrzejewska, M. Pietrzak, J. Pączkowski, Solvent effects on the spectroscopic properties of styrylquinolinium dyes series, J. Fluoresc. 20 (2010) 73–86.
[11] A. Celli, E. Gratton, Dynamics of lipid domain formation: fluctuation analysis, Biochim. Biophys. Acta 1798 (2010) 1368–1376.

[12] S.A. Sánchez, M.A. Tricerri, G. Ossato, E. Gratton, Lipid packing determines protein–membrane interactions: challenges for apolipoprotein AI and high density lipoproteins, Biochim. Biophys. Acta BBA Biomembr. 1798 (2010) 1399–1408.
[13] A.G. Lacko, M. Nair, S. Paranjape, L. Mooberry, W.J. McConathy, Trojan horse meets magic bullet to spawn a novel, highly effective drug delivery model, Chemotherapy (Basel) 52 (2006) 171.
[14] C. Matz, A. Jonas, Micellar complexes of human apolipoprotein AI with phosphatidylcholines and cholesterol prepared from cholate-lipid dispersions, J. Biol. Chem. 257 (1982) 4535.
[15] A. Jonas, Reconstitution of high-density lipoproteins, Meth. Enzymol. 128 (1986) 553–582.
[16] J. Short, J. Roberts, D. Roberts, G. Hodges, S. Gutsell, R. Ward, Practical methods for the measurement of log P for surfactants, Ecotoxicol. Environ. Saf. 73 (2010) 1484–1489.
[17] R. Luchowski, P. Kapusta, M. Szabelski, P. Sarkar, J. Borejdo, Z. Gryczynski, et al., FRET-based picosecond lifetime reference for instrument response evaluation, Meas. Sci. Technol. 20 (2009) 095601.
[18] D. Magde, E. Elson, W. Webb, Thermodynamic fluctuations in a reacting system—measurement by fluorescence correlation spectroscopy, Phys. Rev. Lett. 29 (1972) 705–708.
[19] D. Magde, E.L. Elson, W.W. Webb, Fluorescence correlation spectroscopy. II. An experimental realization, Biopolymers 13 (2004) 29–61.
[20] A. Bajorek, K. Trzebiatowska, B. Jędrzejewska, M. Pietrzak, R. Gawinecki, J. Pączkowski, Developing of fluorescence probes based on stilbazolium salts for monitoring free radical polymerization processes. II, J. Fluoresc. 14 (2004) 295–307.